UNIVERSITY OF AMSTERDAM

UvA-DARE (Digital Academic Repository)

Buckling of liquid columns

Habibi, M.; Rahmani, Y.; Bonn, D.; Ribe, N.M.

DOI
10.1103/PhysRevLett.104.074301
Publication date
2010
Document Version
Final published version
Published in
Physical Review Letters

Link to publication

Citation for published version (APA):
Habibi, M., Rahmani, Y., Bonn, D., & Ribe, N. M. (2010). Buckling of liquid columns. *Physical Review Letters*, *104*(7), 074301. https://doi.org/10.1103/PhysRevLett.104.074301

General rights
It is not permitted to download or to forward/distribute the text or part of it without the consent of the author(s) and/or copyright holder(s), other than for strictly personal, individual use, unless the work is under an open content license (like Creative Commons).

Disclaimer/Complaints regulations
If you believe that digital publication of certain material infringes any of your rights or (privacy) interests, please let the Library know, stating your reasons. In case of a legitimate complaint, the Library will make the material inaccessible and/or remove it from the website. Please Ask the Library: https://uba.uva.nl/en/contact, or a letter to: Library of the University of Amsterdam, Secretariat, Singel 425, 1012 WP Amsterdam, The Netherlands. You will be contacted as soon as possible.

UvA-DARE is a service provided by the library of the University of Amsterdam (https://dare.uva.nl)

Download date:24 Apr 2024

Buckling of Liquid Columns

M. Habibi,[1] Y. Rahmani,[1,2] Daniel Bonn,[2,3] and N. M. Ribe[4]

[1]Institute for Advanced Studies in Basic Sciences, Zanjan 45195-1159, Iran
[2]Van der Waals-Zeeman Institute, University of Amsterdam, Valckenierstraat 65, 1018 XE Amsterdam, The Netherlands
[3]Laboratoire de Physique Statistique, École Normale Supérieure, 24, rue Lhomond, 75231 Paris Cedex 05, France
[4]Laboratoire FAST, Université Pierre et Marie Curie-Paris 6, Université Paris-Sud, CNRS, Bâtiment 502, Campus Universitaire, Orsay 91405, France

(Received 23 July 2009; published 17 February 2010)

Under appropriate conditions, a column of viscous liquid falling onto a rigid surface undergoes a buckling instability. Here we show experimentally and theoretically that liquid buckling exhibits a hitherto unsuspected complexity involving three different modes—viscous, gravitational, and inertial—depending on how the viscous forces that resist bending of the column are balanced. We also find that the nonlinear evolution of the buckling exhibits a surprising multistability with three distinct states: steady stagnation flow, ''liquid rope coiling,'' and a new state in which the column simultaneously folds periodically and rotates about a vertical axis. The transitions among these states are subcritical, leading to a complex phase diagram in which different combinations of states coexist in different regions of the parameter space.

DOI: 10.1103/PhysRevLett.104.074301 PACS numbers: 46.32.+x, 46.70.Hg

The buckling of solids is a classical subject in mechanics. In 1757, Euler showed that an elastic column with diameter d and Young's modulus E buckles when its length exceeds a critical value $\sim(E/P)^{1/2}d$, where P is the force per unit area applied to its end [1]. The behavior of honey falling onto toast shows that liquid columns can also buckle. However, this phenomenon is harder to understand because Young's modulus is zero, whence Euler's formula would incorrectly predict buckling even for zero height.

How can liquid buckling then be understood? A vertical liquid column can be created by ejecting a thin stream of fluid through a hole of diameter d located a distance H above a rigid surface. The stability of this situation was first analyzed theoretically by [2], who predicted that buckling begins when H exceeds d by a critical factor that depends on the magnitudes of surface tension and gravity relative to viscous forces. However, the steady columnar shape analyzed by [2] is infinitely wide at the bottom, and is therefore not realistic. As a result, the analysis misses two additional buckling modes (analyzed below) in which the relevant length scale is not d, but rather the diameter d_1 of the column at the bottom, where $d_1 \ll d$ because gravity thins the fluid stream as it falls.

In this Letter we show that liquid buckling can involve three different modes—viscous, gravitational, and inertial—depending on how the viscous forces that resist the bending of the column are balanced. We characterize these regimes both experimentally and theoretically, and find reasonable agreement between the two. We also investigate the nonlinear evolution of the system after buckling. We find that liquid columns can be multistable, exhibiting three distinct states (stagnation flow, coiling, and rotatory folding) in different combinations depending on the fall height H, the viscosity ν, and the flow rate Q. This is surprising in the light of previous experiments with more viscous fluid columns, in which multistability was either not observed [3–5] or was limited to the coexistence of multiple frequencies within the coiling state [6–10].

Experimental observations.—We used silicone oils with density $\rho = 0.97$ g/cm^3, surface tension $\gamma = 21.5$ dyn/cm, and viscosities $\nu = 330$–2220 cS. The oil fell from a hole of diameter $d = 2$–4 mm in the bottom of a constant-head reservoir onto a horizontal plate 5 cm in diameter a distance $H = 2$–1500 mm below. The flow rate ($Q = 0.08$–0.3 ml/s) was measured by weighing the accumulated oil. Viscosities were measured using a Rheometrics ARES cone-plate rheometer and were independent of strain rate, indicating that the fluids are Newtonian. In a typical series of experiments, ν, d, and Q were constant while H was varied.

We find that the liquid column can exhibit three distinct steady or steady periodic states, depending on the values of the experimental parameters: axisymmetric stagnation flow [S; Fig. 1(h)], liquid rope coiling [C; Fig. 1(f)], and a complex ''rotatory folding'' state [F; Figs. 1(a)–1(d)] that has not been observed previously to our knowledge. The column here folds back upon itself periodically while simultaneously rotating about a vertical axis with a much lower frequency. The images in Figs. 1(a)–1(d) are separated by 1/4 of the rotation period, and show how the overall shape depends on whether the folded structure is viewed perpendicular to [Fig. 1(a)] or parallel to [Fig. 1(c)] its longer lateral dimension.

To identify when the buckling transition from stagnation flow to one of the other two states (C or F) occurs, we map out a phase diagram of our observations as a function of ν, Q, and H. Since a three-dimensional diagram is hard to read, we first show a projection of all our data onto the ν-Q plane (Fig. 2). Different states and combinations of them are observed. The symbol S means that no buckling oc-

 © 2010 The American Physical Society

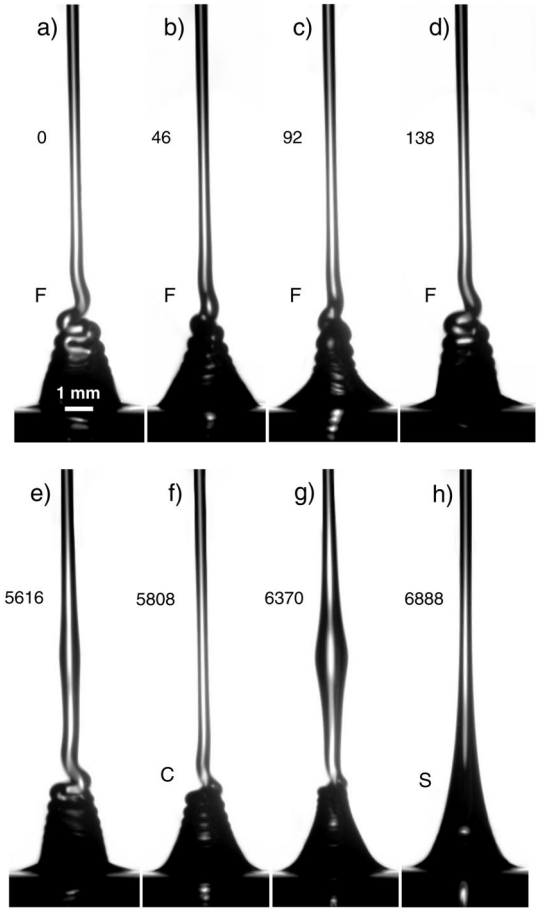

FIG. 1. Time sequence of photographs showing three possible states of a viscous column with $\nu = 946$ cS, $Q = 0.19$ ml/s, $d = 2.6$ mm, and $H = 14$ cm. (a)–(d) Folding with rotation, (f) steady coiling, (h) axisymmetric stagnation flow. Panels (e) and (g) show the finite-amplitude perturbations that trigger the transitions between states. Numbers indicate time in ms.

curred at any height. The symbol C indicates that coiling was the only state observed in the height range $H_1 \leq H \leq H_2$, where $H_1 \leq 2.2$ cm is the height where buckling first occurred, and $H_2 \geq 30$ cm is the height where the column broke up episodically via capillary (Rayleigh) instability. The notations $S + C$, $C + F$, and $S + C + F$ mean that the states indicated were all observed at different times during single experiments at fixed heights in the range $H_1 \leq H \leq H_2$. Figure 1 and the linked video [11] show a continuous time sequence of the three states (in the order $F \rightarrow C \rightarrow S$) at a fixed height. In other experiments, the transitions $C \rightarrow F$, $S \rightarrow C$, $F \rightarrow S$, and $S \rightarrow F$ were also observed. The transitions between states were triggered by finite-amplitude perturbations traveling down the column [Figs. 1(e) and 1(g)], which in most cases were generated by tapping the experimental apparatus lightly.

Figure 3 shows a cross section of the phase diagram at $Q = 0.131$ ml/s, displaying the sequence of states observed as a function of fall height. No buckling occurs at any height for $\nu \leq 474$ cS (green; S). For $\nu \geq 598$ cS, buckling in the form of coiling (C) begins at $H = H_1 =$

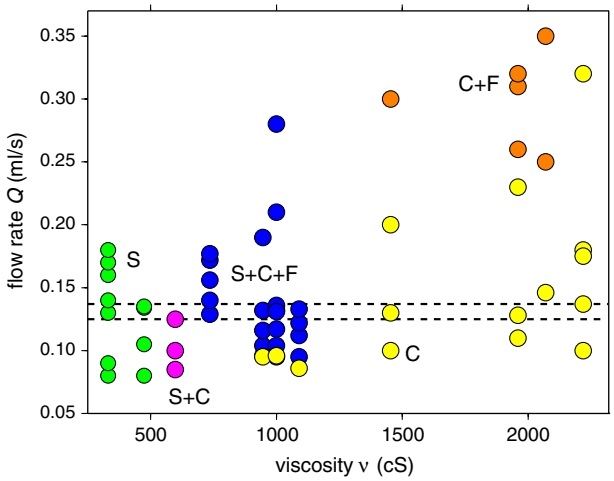

FIG. 2 (color online). Experimentally determined phase diagram in the space (ν, Q). In most cases, the hole diameter was $d = 4$ mm for $\nu \geq 1450$ cS and 2 mm for $\nu \leq 1090$ cS. Experiments with $\nu = 1000$ cS using both hole sizes confirm that the phase diagram is independent of d. The dashed lines indicate the range of values of Q used in Fig. 3.

1.5–2.3 cm (green to yellow; S to C). C is then the sole state observed up to a maximum height (4.2–100 cm) that increases with viscosity (yellow; C). For still greater heights and $\nu = 598$–1090 cS, C coexists with S (purple; $S + C$) or $S + F$ (blue; $S + C + F$). Finally, the column becomes unstable to capillary breakup (red; B) when H exceeds a value $H_2 = 30$–135 cm that increases with the viscosity.

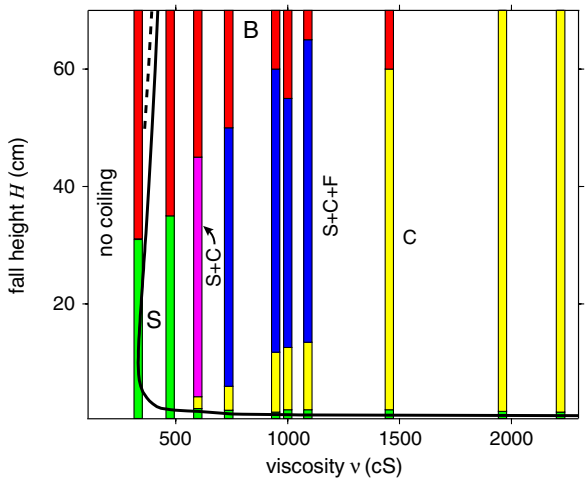

FIG. 3 (color online). Cross section $Q = 0.131 \pm 0.006$ ml/s of the experimental phase diagram (Fig. 2), expanded in the third (H) dimension. Red (upper left, symbol B) indicates capillary breakup, and the remaining colors are as in Fig. 2. Solid line: Numerically calculated coiling cessation surface separating regions where coiling solutions exist (above or to the right) and do not exist (below or to the left). Dashed line: Coiling cessation surface (uppermost portion only) in the limit of zero surface tension.

The phase diagram shows that multiple states can exist for identical experimental conditions. Figure 4 shows the angular frequencies (Ω) of coiling (C), folding (F), and rotation of the folding column (R) as a function of H for an experiment with $d = 2$ mm, $\nu = 950$ cS, and $Q = 0.132$ ml/s, determined by counting frames in movies taken with a rapid camera. Coiling begins at $H = H_1 = 1.6$ cm and persists up to $H = H_2 = 60$ cm. Folding is observed only for $H \geq 11.8$ cm. Its frequency is about 10% less than the coiling frequency, and the frequency of the simultaneous rotation is a factor of 25–35 smaller still. The coiling frequency predicted numerically for the same parameters using the method of [6] (solid line) agrees well with the experimental measurements. For comparison, the dashed line shows the coiling frequency predicted in the same way but without surface tension.

Onset and cessation of coiling: Theoretical analysis.—Figures 2 and 3 show that buckling first occurs in the form of coiling when both the fall height and the viscosity are sufficiently large (roughly $H > 2.4$ cm and $\nu > 450$ cS), indicating the existence of a critical surface in the (H, ν, Q, d) parameter space. We now investigate the shape of this surface using a mathematical model for a thin liquid filament with inertia subject to gravitational, viscous, and surface tension forces [6]. One possible approach [2] would be to analyze the stability of a steady axisymmetric stagnation flow to small perturbations to determine the critical coiling onset surface. Unfortunately, no steady stagnation state exists if the plate onto which the fluid falls is impermeable. The only way to make the flow steady is to allow the fluid to traverse the plate with a velocity $4Q/(\pi d_1^2)$, where d_1 is the diameter of the column at the plate. Such a basic state is not realistic, and moreover introduces an undesirable free parameter (d_1).

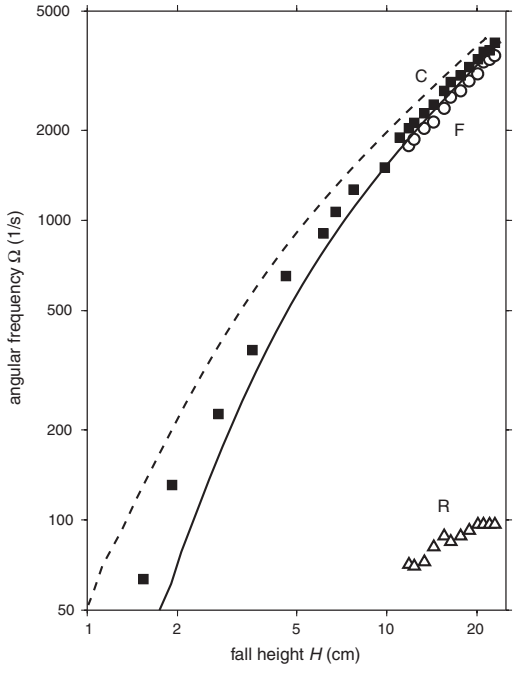

FIG. 4. Angular frequencies of coiling (C, solid squares), folding (F, open circles), and rotation of the folding plane (R, open triangles) as a function of height for an experiment with $d = 2$ mm, $\nu = 946$ cS, and $Q = 0.132$ ml/s. Solid line: Numerical prediction of the coiling frequency using the method of [6]. Dashed line: Same, but without surface tension.

To avoid these difficulties, we proceed "in reverse" by starting from a finite-amplitude coiling solution and then using a continuation procedure [6] to locate the "coiling cessation surface" in the (H, ν, Q, d) space where the solution ceases to exist. The coiling cessation surface need not coincide with the coiling onset surface determined by a traditional linear stability analysis. Our numerical procedure relies on the fact that the coiling frequency Ω_C is double-valued for (H, ν, Q, d) sufficiently close to the cessation surface. The two branches meet in a turning point beyond which no coiling solution exists, and which can be located numerically by continuing a solution on either branch toward the fold until the derivative of the principal continuation parameter (typically H or ν) changes sign. Neglecting surface tension for the moment in order to determine clean scaling laws, we find that the coiling cessation surface has three asymptotic limits corresponding to three modes of coiling cessation: "viscous" (V), "gravitational" (G), and "inertial" (I).

In both the V and G modes, inertia is negligible. Coiling ceases when $H < F(\Pi)d$, where $\Pi = (\nu Q/gd^4)^{1/4}$ and $F(\Pi)$ is shown in Fig. 5(a). The V mode corresponds to the limit $\Pi \gg 1$, in which gravity is negligible and the column diameter $\approx d$ everywhere. Coiling ceases when

$$H < 3.49d \equiv H_V. \tag{1}$$

In the G mode ($\Pi \leq 0.5$), gravity strongly stretches the column, and coiling ceases when

$$H < 5.4(\nu Q/g)^{1/4} \equiv H_G. \tag{2}$$

When H exceeds the critical values H_V or H_G, we recover the well-studied viscous and gravitational regimes, respectively, of finite-amplitude coiling [6,7].

In the I (inertial) mode, coiling ceases when

$$\nu < 0.665(gHQ^2)^{1/4} \equiv \nu_I. \tag{3}$$

Physically, (3) means that coiling ceases when the diameter D of the coiled part of the column becomes comparable to the diameter d_1 of the column itself. Consider a coiling column with H sufficiently large that inertia is important in both the lowermost (coiled) part of the column and the nearly vertical "tail" above it. In the coil, inertia is balanced by viscous forces, so $D \sim (\nu d_1^4/Q)^{1/3}$ [5]. In the tail, by contrast, inertia is balanced by gravity (free fall), implying $d_1 \sim (Q^2/gH)^{1/4}$. Therefore D becomes comparable to d_1 when ν drops below $\sim(gHQ^2)^{1/4}$, in agreement with (3). This analysis is further confirmed by the visually obvious fact [Fig. 5(b)] that $D \approx d_1$ in numerical solutions of steady coiling with $\nu = \nu_I$ [12].

Onset and cessation of coiling: Theory versus experiment.—We consider first the limit in which both inertia and

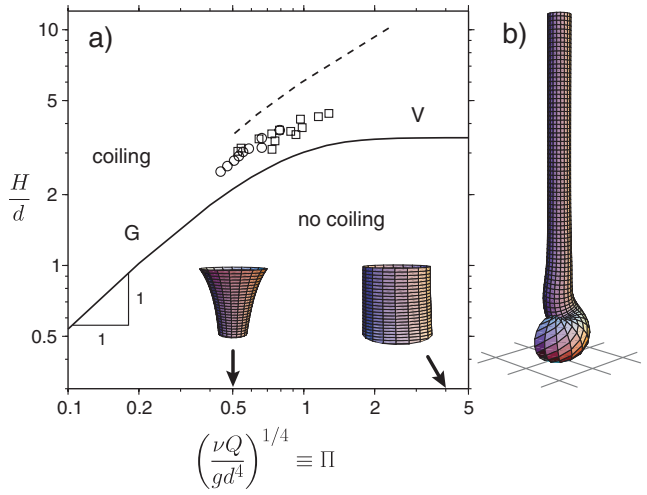

FIG. 5 (color online). (a) Cessation of steady coiling in the inertia-free limit. Solid line: Coiling cessation surface $H/d = F(\Pi)$ separating regions where steady coiling solutions without surface tension exist (above) and do not exist (below). The portions corresponding to the V and G modes are indicated. Dashed line: Coiling onset surface in the absence of surface tension [2]. Symbols: Experimentally measured critical heights [3] for silicone oil with $\gamma/\rho g d^2 = 0.0063$ (circles) and 0.014 (squares). Images: Shapes of the upper part of the column for $H/d = 4$ and the values of Π indicated by the arrows. (b) Numerically determined shape of the lower part of a column coiling in the inertial limit with the critical viscosity $\nu = \nu_I$, for $\Pi = 1.0$ and $H = 40(\nu^2/g)^{1/3}$. The width of each grid square on the bottom surface is $2(Q^2/gH)^{1/4}$.

surface tension are negligible, corresponding to the V and G modes of Fig. 5(a). Experiments in this limit, which require small values of the dimensionless surface tension parameter $\gamma/\rho g d^2$, were performed by [3]. The symbols in Fig. 5(a) show the critical heights measured by [3] for $\gamma/\rho g d^2 = 0.0063$ and 0.014. They lie roughly midway between our coiling cessation surface (solid line) and the coiling onset surface of [2] (dashed line).

To compare our theoretical predictions with our own experiments, in which surface tension cannot be neglected ($\gamma/\rho g d^2 \in [0.14, 0.56]$), we recalculate the coiling cessation surface using the "reverse" continuation procedure described above but with surface tension included. The cross section $Q = 0.13$ ml/s of that surface is shown by the solid black line in Fig. 3. It separates regions where coiling solutions exist (above or to the right) and do not exist (below or to the left). Apart from the additional effect of surface tension, the nearly horizontal portion of the curve ($H < 2.5$ cm) corresponds to the G mode of coiling cessation, and the nearly vertical portion ($\nu < 500$ cS) to the I mode. The critical viscosity $\nu_I = 0.665(gHQ^2)^{1/4}$ for the "pure" (zero surface tension) I mode is shown by the dashed line at the upper left for comparison.

The coiling cessation surface in Fig. 3 agrees with the experiments in the sense that coiling (C) is never observed in the "no coiling" region below or to the left of it. However, the observed cessation of coiling does not coincide with the calculated coiling cessation surface, but instead occurs somewhat above or to the right of it. At the lower left of Fig. 3, for example, the coiling cessation surface underpredicts the observed critical viscosity, which lies somewhere in the range 474–598 cS, by 19%–44%. The critical heights in the G mode (bottom center and right) are also underpredicted, as we saw previously in Fig. 5(a) for the data of [3]. One possible cause of these discrepancies is hysteresis in the buckling transition, which seems to be suggested by the noncoincidence of the coiling onset surface (dashed line) and the coiling cessation surface (solid line) in Fig. 5(a). We attempted to measure hysteresis by first increasing and then decreasing the fall height through the buckling transition, but the result was inconclusive. Another possibility is that the "slender filament" equations used in most numerical coiling models [2,6] are somewhat less accurate when the filament is "thick" [e.g., Fig. 5(b)]. Whatever the reason, we find it encouraging that the theory predicts well the overall trend of the observations, including the sharp transition between the "critical height" and "critical viscosity" portions of the surface where coiling ceases (Fig. 3).

This work was supported by SEDIT/INSU, CISSC, and the French embassy in Tehran. We thank H. Khalesifard, M. Khajepour, and A. Javadi for their help, and two anonymous referees for careful reviews. LPS de l'ENS is UMR 8550 of the CNRS.

[1] L. D. Landau and E. M. Lifshitz, *Theory of Elasticity* (Pergamon, Oxford, 1970), 2nd ed.
[2] B. Tchavdarov, A. L. Yarin, and S. Radev, J. Fluid Mech. **253**, 593 (1993).
[3] J. O. Cruickshank, Ph.D. thesis, Iowa State University, 1980.
[4] J. O. Cruickshank and B. R. Munson, J. Fluid Mech. **113**, 221 (1981).
[5] L. Mahadevan, W. S. Ryu, and A. D. T. Samuel, Nature (London) **403**, 502 (2000).
[6] N. M. Ribe, Proc. R. Soc. A **460**, 3223 (2004).
[7] M. Maleki, M. Habibi, R. Golestanian, N. M. Ribe, and D. Bonn, Phys. Rev. Lett. **93**, 214502 (2004).
[8] N. M. Ribe, H. E. Huppert, M. Hallworth, M. Habibi, and D. Bonn, J. Fluid Mech. **555**, 275 (2006).
[9] N. M. Ribe, M. Habibi, and D. Bonn, Phys. Fluids **18**, 084102 (2006).
[10] M. Habibi, M. Maleki, R. Golestanian, N. Ribe, and D. Bonn, Phys. Rev. E **74**, 066306 (2006).
[11] See supplementary material at http://link.aps.org/supplemental/10.1103/PhysRevLett.104.074301 for a movie. Each frame is 1 cm wide, and the playback rate is 1/20 real time.
[12] The criterion $Q/\nu d > 1$ for the cessation of inertial coiling [4] incorrectly implies that d is the relevant length scale when inertia is dominant. In fact, the column diameter $d_1 \sim (Q^2/gH)^{1/4}$ at the bottom is the relevant length scale.